Journal of Bone Oncology 28 (2021) 100360

Contents lists available at ScienceDirect

Journal of Bone Oncology

journal homepage: www.elsevier.com/locate/jbo

Hsa_circ_0010220 regulates miR-198/Syntaxin 6 axis to promote osteosarcoma progression

Zhaoan Lu *, Chuanwen Wang, Xiaolong Lv, Wen Dai

Department of Orthopedics, the First People's Hospital of Shangqiu City, Shangqiu 476100, Henan, China

ARTICLE INFO

Article history:
Received 28 December 2020
Revised 24 March 2021
Accepted 25 March 2021
Available online 22 April 2021

Keywords:
Osteosarcoma
Hsa_circ_0010220
miR-198
STX6

ABSTRACT

Background: Circular RNAs (circRNAs) are a class of endogenous RNAs that are involved in osteosarcoma progression. Hsa_circ_0010220 (circ_0010220) is a circRNA generated by gene Rho Guanine Nucleotide Exchange Factor 10 Like (ARHGEF10L) and is upregulated in osteosarcoma, but its functional role in osteosarcoma is limited studied. This study aimed to illustrate the regulatory mechanism underlying circ_0010220 in osteosarcoma.

Methods: 51 paired tumor and normal tissues were obtained from osteosarcoma patients. circ_0010220, microRNA (miR)-198 and Syntaxin 6 (STX6) abundances were examined by quantitative reverse transcription polymerase chain reaction and western blot. Cell proliferation, cell cycle, apoptosis, migration and invasion were analyzed via Cell Counting Kits-8 (CCK-8), colony formation, flow cytometry and transwell analyses. Target relationship was verified via dual-luciferase reporter analysis, RNA immunoprecipitation and pull-down. The *in vivo* function was analyzed using a xenograft model.

Results: Circ_0010220 was elevated in osteosarcoma tissues and cells, and was related to the lower survival rate of osteosarcoma patients. Circ_0010220 knockdown inhibited cell proliferation, migration and invasion, but induced cell cycle arrest and apoptosis *in vitro*. Besides, circ_0010220 silence curbed the growth of xenograft osteosarcoma tumors *in vivo*. Mechanistic research revealed that miR-198 is a target of circ_0010220, and directly targets STX6. Moreover, circ_0010220 upregulated the expression of STX6 by sponging miR-198 to regulate cell proliferation, migration, invasion, cell cycle, and apoptosis.

Conclusion: Circ_0010220 contributes to osteosarcoma progression through mediating miR-198/STX6 axis, which might be a novel therapeutic target for osteosarcoma therapy.

1. Introduction

Osteosarcoma, a primary bone malignancy emerged from mesenchymal cells, is the main form of emerging from mesenchymal cells with high incidence and mortality [1,2]. The main characteristics of osteosarcoma are the formation of osteoid tissue, abnormal growth of bone-related mesenchymal cells, and the highly aggressive phenotype, nearly 20% of osteosarcoma patients had tumor metastasis, including commonly to the lungs followed by additional bone, lymph node or other soft tissue lesions [2,3]. The 5-year survival rate of osteosarcoma patients, who were diagnosed with metastatic or recurrent tumors, is below 30% [4]. Despite multiple treatments including surgery, chemotherapy, and radiotherapy have been applied in clinical, the limited efficacy and serious side effects demand us a deep understanding of the regulatory mechanism underlying osteosarcoma initiation and progression to find novel treatment strategies for osteosarcoma.

Circular RNAs (circRNAs), a distinct group of noncoding RNAs, are generated via back-splicing of covalently joined 3′- and 5′-ends without the polyadenylated tail [5]. Different from their linear transcripts, the special closed-ring structure of circRNAs allows it to be more stable and hardly degraded by RNA exonuclease [6,7]. A number of studies have disclosed the relationship between uncontrolled expression of circRNAs and the tumorigenesis of multiply cancers, including osteosarcoma [8–11]. Besides, circRNAs are involved in the pathogenesis of osteosarcoma, and have enormous potential as prognostic and diagnostic biomarkers for osteosarcoma [12,13]. For example, hsa_circ_0003732 promoted osteosarcoma cell proliferation via regulating miR-545 and Cyclin A2 [14]. Furthermore, hsa_circ_0005909 and hsa_circ_0000073 could promote osteosarcoma cell proliferation, migration and invasion via modulating different miRNAs [15,16]. According to the GSE140256 dataset, circRNA hsa_circ_0010220 (circ_0010220)

* Corresponding author at: Department of Orthopedics, The First People's Hospital of Shangqiu City, No. 292, Kaixuan South Road, Shangqiu City, Henan, China.
E-mail address: luzhaoan321@163.com (Z. Lu).

https://doi.org/10.1016/j.jbo.2021.100360
2212-1374/

expression is up-regulated in 3 cases of osteosarcoma tumor tissues in contrast to adjacent normal tissues. Circ_0010220, originated from the Rho Guanine Nucleotide Exchange Factor 10 Like (ARHGEF10L) gene, is located at chromosome 12: 17907047-18024370. Besides, a recent research uncovered that circ_0010220 mediated the progression tumorigenesis of osteosarcoma via miR-503-5p/CDCA4 axis [17]. However, the function of circ_0010220 in osteosarcoma progression still need further investigation.

Functionally, circRNAs could function as a competitive endogenous RNA (ceRNA) for microRNAs (miRNAs) to regulate the downstream mRNAs with the crosstalk of miRNAs, thereby exerting various effects on cell proliferation, apoptosis and metastasis [18,19]. The ceRNA network including circRNAs, miRNAs and mRNAs, could competitive bind to the same miRNA response elements (MREs) to regulate each other [20]. A growing evidence has disclosed that ceRNA networks have a critical role in osteosarcoma progression [21,22]. For example, circ-03955 acted as miR-3662 sponge to regulate the expression of MTDH, thus suppressed the growth and metastasis of osteosarcoma [22]. And circ-0001785 upregulated HOBX2 expression by acting as a ceRNA for miR-1200 to regulate the PI3K/Akt signaling and Bcl-2 family pathway in osteosarcoma [23]. Thus, it is necessary to elucidate the function of circRNA-mediated ceRNA network in osteosarcoma tumorigenesis and progression.

In current research, we investigated the role of circ_0010220 in osteosarcoma progression by detecting its effect on cell proliferation, cycle process, apoptosis, migration and invasion. Moreover, we further investigated the regulatory mechanism underlying circ_0010220 in osteosarcoma progression. Our research might provide the novel prognostic and therapeutic targets for osteosarcoma.

2. Materials and methods

2.1. Bioinformatics analysis

The data of circ_0010220 expression level in osteosarcoma tissues was approved by GSE140256 dataset from Gene Expression Omnibus (GEO) database (http://www.ncbi.nlm.nih.gov/geo/), which conducted the microarray profiling analysis of circRNAs in osteosarcoma tumors and adjacent normal tissues derived from three primary osteosarcoma patients who underwent complete resection without pre- or postoperative chemotherapies. The binding site of circ_0010220 and miR-198 was predicted via Circinteractome (http://circinteractome.nia.nih.gov/). The potential targets of miR-198 was predicted via bioinformatics software TargetScan (http://www.targetscan.org/vert_71/).

2.2. Patients and tissues

The paired osteosarcoma tumor tissues and adjacent normal tissues were harvested from 51 patients who were diagnosed as osteosarcoma at the First People's Hospital of Shangqiu City. None of the patients received radio- or chemo-therapy before surgery. All patients have signed the written informed consent, and authorized the use of the tissues for the intended experiments. All of the patients were followed for a total of 60-months to determine survival status. This research was in accordance with the Helsinki Declaration, and was approved by the ethics committee of the First People's Hospital of Shangqiu City.

2.3. Cell culture

The osteosarcoma cell lines HOS and U2OS cells and normal osteoblast cell line hFOB 1.19 cells were purchased from Procell Life Science Technology (Wuhan, China). Cells were grown in minimum Eagle's medium (Procell Life Science Technology) adding with 10% fetal bovine serum (Gibco, Gran Island, NY, USA) and 1% penicillin/streptomycin (Beyotime, Shanghai, china) at 5% CO_2 and 37 °C. hFOB 1.19 cells were cultured under same condition plus 0.3 mg/mL G418 (Procell Life Science Technology).

2.4. Cell transfection

Circ_0010220 overexpression vector was constructed by Geneseed (Guangzhou, China) based on the pCD5-ciR vector (Geneseed), and the pCD5-ciR vector alone was used negative control (circ-NC). STX6 overexpression vector was constructed via Genomeditech (Shanghai, China) with the pcDNA3.1 vector (Genomeditech) as negative control (pcDNA). Small interfering RNA (siRNA) for circ_0010220 (si- circ_0010220#1, si-circ_0010220#2 and si-circ_0010220#3), siRNA negative control (si-NC), miR-198 mimic, miR-198 inhibitor (anti-miR-198), and negative control (NC or anti-NC) were generated by Ribobio (Guangzhou, China). The oligonucleotide sequences were exhibited in Table 1. HOS and U2OS cells were transfected with 1 μg vectors or 30 nM oligonucleotides using Lipofectamine 2000 (Thermo Fisher Scientific, Waltham, MA, USA) for 24 h. 24, 48 or 72 h upon transfection, cells were collected for further research.

2.5. Quantitative reverse transcription polymerase chain reaction (RT-qPCR)

RNA was isolated from osteosarcoma tissues and cells using Trizol (Takara, Otsu, Japan) reagent. To analyze the stability of circRNA, RNA was incubated with 3 U/μg RNase R (Geneseed) for 30 min. The RNA in nuclear or cytoplasm was extracted with a Cytoplasmic and Nuclear RNA Purification kit (Norgen Biotek, Thorold, Canada). For RT-qPCR analysis, 800 ng RNA was reversely transcribed to complementary DNA using the miRNA or mRNA Reverse Transcriptase kit (Takara). The qPCR analysis was conducted using SYBR RT-PCR Quick Master Mix (Toyobo, Tokyo, Japan) with the following amplification protocol: 95 °C for 5 min, 40 cycles of 95 °C for 15 s, and 60 °C for 1 min. The primer sequences were synthesized by Sangon (Shanghai, China) and shown in Table 2. U6 or 18S was used as internal normalization control. Relative RNA level was analyzed by $2^{-\Delta\Delta Ct}$ method.

2.6. Cell Counting Kits-8 (CCK-8)

Cell proliferation was evaluated via CCK-8 and colony formation analyses. For CCK-8 analysis, 1×10^4 HOS and U2OS cells were placed into the 96-well plates. After incubation for 24, 48 or 72 h, 10 μL CCK-8 reagent (Solarbio, Beijing, China) was added to every well. After continuous culture for 3 h, the optical density (OD) value was measured with a microplate reader (Bio-Rad, Hercules, CA, USA) at 450 nm.

Table 1
The oligo sequences for transfection in this study.

Name	Sequence (5'-3')
si-circ_0010220#1	UACACACUCCAAGUCCAGAUG
si-circ_0010220#2	UCCCAGCUACACACUCCAAGU
si-circ_0010220#3	CACACUCCAAGUCCAGAUGUA
si-NC	AUGUGACUCCAAGUCCAGAUG
miR-198 mimic	GGUCCAGAGGGGAGAUAGGUUC
NC	CGAUCGCAUCAGCAUCGAUUGC
anti-miR-198	GAACCUAUCUCCCCUCUGGACC
anti-NC	CUAACGCAUGCACAGUCGUACG

Table 2
The primer sequences for RT-qPCR in this study.

Name	Sequence (5′-3′)	
	Forward	Reverse
miR-198	GCCGAGGGTCCAGAGGGGAGA	AGTGCAGGGTCCGAGGTATT
U6	CTCGCTTCGGCAGCACATATACT	ACGCTTCACGAATTTGCGTGTC
circ_0010220	TCTGGGAGATGCTGGAATAAA	ATCTCCTATGGCAGGCTGTG
ARHGEF10L	CTGTGTGAGACGTTGACGGA	TGGTTGGCAGGCTTGAAGTT
STX6	AGGAGAGGTACAGAAAGCAGTCA	TGTCCCTGACAACTTGCCGA
18S	ACCCGTTGAACCCCATTCGTGA	GCCTCACTAAACCATCCAATC
IGF1R	CCTGCACAACTCCATCTTCGTG	CGGTGATGTTGTAGGTGTCTGC
TRIM44	GCCAGGAAGATAGGCAGCTCAT	CTTCAGTCCACCTGAGTCTTTGC
SOX5	CTCGGCAAATGAAGGAGCAACTC	ACTGCCAGTTGCTGAGTCAGAC
WNT7B	AGAAGACCGTCTTCGGGCAAGA	AGTTGCTCAGGTTCCCTTGGCT
TGM2	TGTGGCACCAAGTACCTGCTCA	GCACCTTGATGAGGTTGGACTC
XIAP	TGGCAGATTATGAAGCACGGATC	AGTTAGCCCTCCTCCACAGTGA
IKBKB	ACAGCGAGCAAACCGAGTTTGG	CCTCTGTAAGTCCACAATGTCGG

2.7. Colony formation assay

For the colony formation assay, 3×10^2 HOS and U2OS cells were inoculated into 6-well plates and cultured for 10 days with a medium change every two days. Subsequently, cells were fixed and stained with 0.1% crystal violet (Solarbio). The visible colonies were photographed, and relative colony formation was analyzed by normalizing the control group.

2.8. Flow cytometry

Cell cycle distribution and apoptosis were determined using flow cytometry. For cell cycle distribution assay, 2×10^5 HOS and U2OS cells were placed into 12-well plates. Cells were cultured in non-serum medium for 24 h, and next cultured in medium containing 10% serum for 72 h. Then cells were fixed with 75% ethanol (Aladdin, Shanghai, China) and stained with 5 μL propidium iodide (PI; Solarbio). Cell cycle was measured through a flow cytometer (Beckman Coulter, Brea, CA, USA).

Cell apoptosis was examined with an Annexin V-fluorescein isothiocyanate (FITC) apoptosis detection kit (Solarbio). 2×10^5 HOS and U2OS cells were inoculated into 12-well plates for 72 h. Then the cells were harvested and resuspended in Annexin V binding buffer, followed by staining with 10 μL Annexin V-FITC and PI for 5 min. Next, cell apoptosis was examined with a flow cytometer. The ratio of apoptotic cells was expressed as the percentage of cells with Annexin V-FITC$^+$ and PI$^{+/-}$.

2.9. Transwell analysis

Cell migration and invasion were measured using 24-well transwell chambers (Corning, Corning, NY, USA). For invasion analysis, 2×10^5 HOS and U2OS cells in medium without serum were placed into the upper chamber pre-coated with Matrigel (Solarbio); for migration analysis, 1×10^5 cells in non-serum medium were added into the upper chamber with fibronectin-coated polycarbonate membrane. The low chamber was added with 500 μL medium plus 10% serum. After incubation for 24 h, cells were fixed and then dyed to 0.1% crystal violet. The migratory or invasive cells were photographed with a 100 × magnification microscope (Nikon, Tokyo, Japan). The cell number was counted with 3 random fields by Image J v1.8 (NIH, Bethesda, MD, USA).

2.10. Dual-luciferase reporter analysis

The sequences of circ_0010220 or 3′ UTR of STX6 contained wild type (wt) or mutant type (mut) miR-198 binding sites were cloned into the pGL3 vector (Promega, Madison, WI, USA) to construct the luciferase reporter vectors, and named as circ_0010220- wt, STX6-wt, circ_0010220-mut or STX6-mut. The luciferase reporter vector and miR-198 mimic or NC were co-transfected into HOS and U2OS cells using Lipofectamine 2000. 24 h upon transfection, the luciferase activity was measured via a dual luciferase reporter assay system (Promega).

2.11. RNA immunoprecipitation (RIP) assay

RIP analysis was conducted with a Magna RIP kit (Sigma, St. Louis, MO, USA). 1×10^7 HOS and U2OS cells were lysed, and the lysate was interacted with 50 μL beads coated with argonaute 2 antibody (anti-Ago2) or IgG antibody (anti-IgG) overnight. The IgG was used as a negative control. The enrichment of circ_0010220, miR-198 or STX6 was detected by RT-qPCR.

2.12. RNA pull-down assay

RNA pull-down assay was conducted using a Magnetic RNA-protein pull-down kit (Thermo Fisher Scientific). 1×10^7 HOS and U2OS cells were lysed in the standard lysis buffer, and incubated with Bio-miR-198 or negative control (Bio-NC) for 8 h. Then the RNA-RNA complex were conjugated with 50 μL streptavidin magnetic beads. After elution, circ_0010220 level was examined by RT-qPCR.

2.13. Western blot

Total protein of osteosarcoma tissues and cells was isolated in RIPA buffer (Thermo Fisher Scientific), and the concentration of protein was detected using the BCA protein assay kit (Beyotime). 30 μg protein was separated using 10% sodium dodecyl sulphate-polyacrylamide gel electrophoresis, and transferred onto the polyvinylidene fluoride membranes (Bio-Rad). Followed by blocking the membrane with 5% fat-free milk. Then the membrane was incubated with primary antibodies against STX6 (ab243719, 1:5000 dilution, Abcam, Cambridge, UK), proliferating cell nuclear antigen (PCNA) (ab15497, 1:2000 dilution, Abcam) or β-Actin (ab115777, 1:2000 dilution, Abcam) overnight and horseradish peroxidase-labeled secondary antibody IgG (ab97080, 1:20000 dilution, Abcam) for 2 h. β-Actin was used as an internal control. The blots were visualized using enhanced chemiluminescence reagent (Thermo Fisher Scientific), and analyzed by Image J v1.8 software.

2.14. Murine xenograft model

Ten BALB/c athymic mice (male, 4-week-old) were obtained from Charles River Laboratories (Beijing, China). The lentiviral vector of short hairpin RNA against circ_0010220 (Lenti-sh-circ_0010220) and negative control (Lenti-sh-NC) were constructed by Genomeditech. U2OS cells were infected with Lenti-sh-circ_0010220 or Lenti-sh-NC, then the stable transduced U2OS cells were selected using (1 μg/ml) puromycin. 3×10^6 stable U2OS cells were subcutaneously injected into the right armpit of the athymic mice (n = 5/group). Tumor growth was monitored every five days for 6 times, and tumor volume was calculated via the formula ($1/2 \times \text{length} \times \text{width}^2$). After 30 days, mice were euthanized using 5% isoflurane. Tumor samples were harvested, and tumor weight was examined at the end point. Circ_0010220, miR-198, STX6 and PCNA levels in tumor samples were detected by RT-qPCR or western blot. The animal experiments were conducted with the guidance of the care and use of Laboratory animals published by National Institutes of Health, and were approved by the Institutional Animal Ethics Committee of the First People's Hospital of Shangqiu City.

2.15. Statistical analysis

Each experiment was repeated three times, and the results were shown as mean ± standard deviation (SD). The data was analyzed by SPSS v18.0 software (SPSS, Chicago, IL, USA). The correlation between miR-198 and circ_0010220 or STX6 in tumor tissues was determined via the Pearson's correlation coefficient. The difference was evaluated using Student *t*-test (for 2 groups) or analysis of variance (ANOVA) followed via Tukey's or Sidak's post hoc test (for multiple groups). $P < 0.05$ was considered as statistical difference.

3. Results

3.1. Circ_0010220 expression is elevated in osteosarcoma tissues and cells

According to the GSE140256 dataset, circ_0010220 expression was elevated in osteosarcoma tumor tissues in comparison with adjacent normal tissues (Fig. 1A). Next, we further verified the expression of circ_0010220 in osteosarcoma tumor tissues and cells. As expected, circ_0010220 was upregulated in 51 cases of osteosarcoma tumor (Fig. 1B), as well as in osteosarcoma cell line (HOS and U2OS) (Fig. 1C) in contrast with the adjacent normal samples and human osteoblast cell line (hFOB 1.19). Additionally, circ_0010220 was mainly located in the cytoplasm of HOC and U2OS cells (Fig. 1D), and was resistant to RNase R digestion than its linear transcript (ARHGEF10L) (Fig. 1E). Furthermore, the osteosarcoma patients were divided into circ_0010220 high expression (n = 25) and low expression (n = 26) group according to the median value of circ_0010220 in osteosarcoma tissues. After a 60-months follow-up, patients with high circ_0010220 expression group had lower survival rate than those with low circ_0010220 expression group (Fig. 1F). These results showed that circ_0010220 was upregulated in osteosarcoma tissues and cells, and was associated with the overall survival of osteosarcoma patients.

3.2. Circ_0010220 knockdown inhibites cell proliferation, migration and invasion, but induces cell cycle arrest and apoptosis in vitro

To investigate the function of circ_0010220 on osteosarcoma progression *in vitro*, we knocked down the expression of circ_0010220 in HOS and U2OS cells using siRNAs transfection. As shown in Fig. 2A, all of the siRNAs that targeted the junction site of circ_0010220 significantly suppressed circ_0010220 expression. And si-circ_0010220#1 was used as further experiments due to its

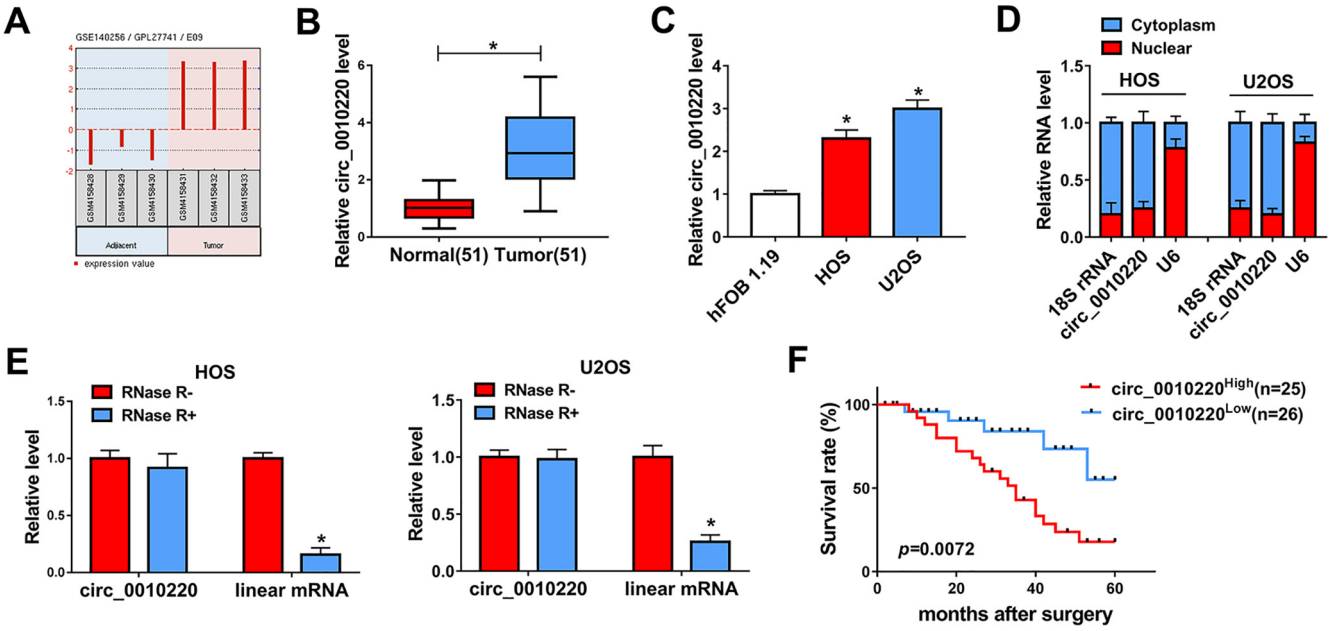

Fig. 1. Circ_0010220 expression in osteosarcoma tumor and cells. (A) Circ_0010220 expression level in osteosarcoma tumor tissues (n = 3) and adjacent normal tissues (n = 3) based on the data of circRNA microarray profiling dataset (GSE140256). (B) Circ_0010220 expression was detected via RT-qPCR in 51 paired human osteosarcoma tumor tissues and adjacent normal tissues (n = 51). (C) Relative expression of circ_0010220 in OS cell lines (HOS and U2OS) and hFOB 1.19 cells was examined by RT-qPCR. (D) Subcellular distribution analysis of circ_0010220 in HOS and U2OS cells. (E) The levels of circ_0010220 and its linear transcript in HOS and U2OS cells with or without RNase R incubation were detected by RT-qPCR. (F) Kaplan-Meier analysis for the survival rate of patients with high or low circ_0010220 expression. *$P < 0.05$.

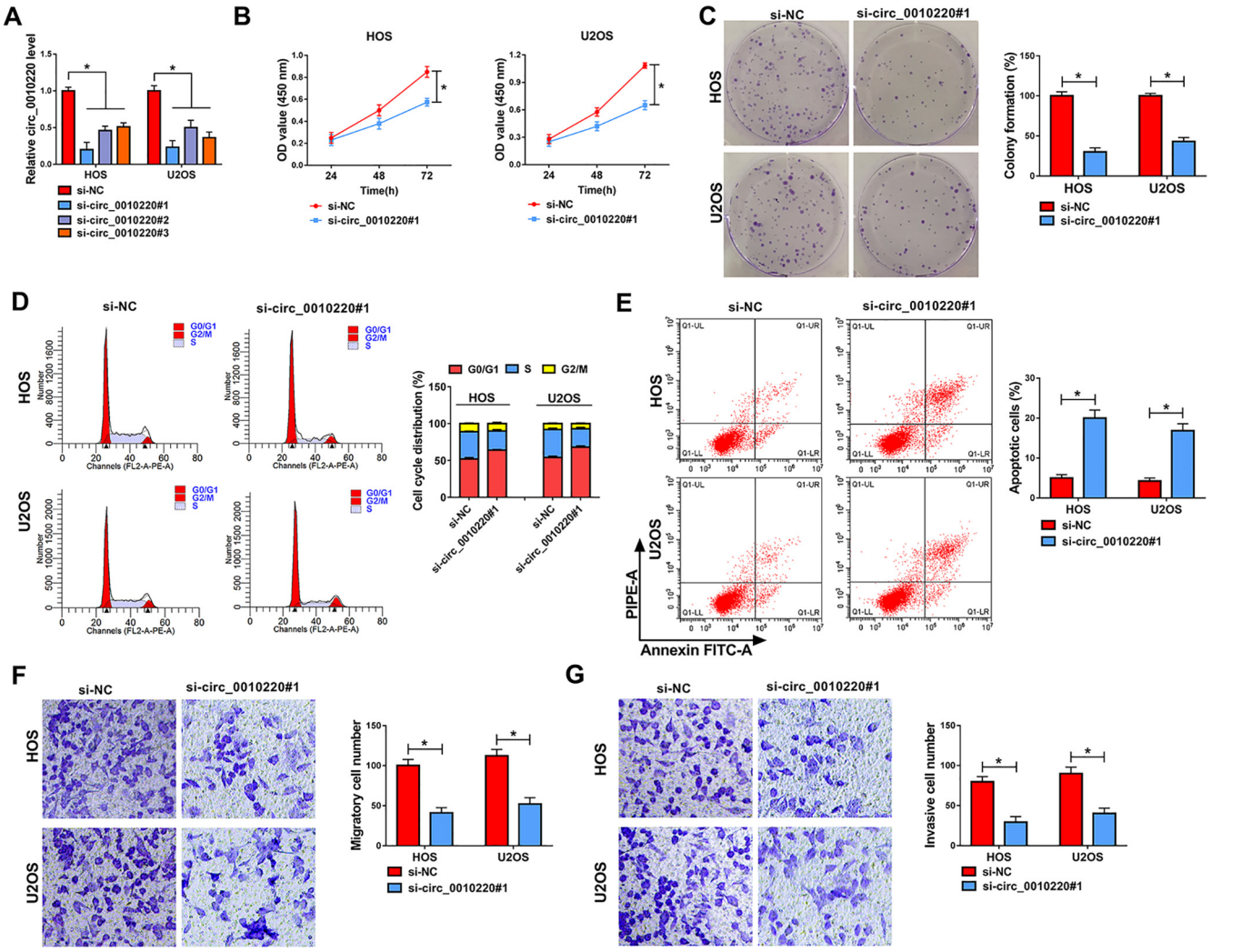

Fig. 2. Circ_0010220 knockdown suppressed the proliferation, migration, and invasion, but induced cell cycle arrest and apoptosis in osteosarcoma cells. (A) Circ_0010220 level was measured in cells transfected with si-circ_0010220#1, si-circ_0010220#2, si-circ_0010220#3 or si-NC. (B) Cell proliferation was detected via CCK-8 in cells transfected with si-circ_0010220#1 or si-NC. (C) Colony formation efficiency was analyzed in cells transfected with si-circ_0010220#1 or si-NC. (D and E) Cell cycle distribution and apoptosis were measured via flow cytometry in cells transfected with si-circ_0010220#1 or si-NC. (F and G) Cell migration and invasion were examined via transwell assay in cells transfected with si-circ_0010220#1 or si-NC. $^{*}P < 0.05$.

highest knockdown efficacy. CCK-8 and colony formation assay uncovered that circ_0010220 knockdown significantly decreased cell proliferation (Fig. 2B and C). Moreover, circ_0010220 knockdown induced cell cycle arrest at G0/G1 phase and promoted apoptosis in osteosarcoma cells (Fig. 2D and E). Additionally, circ_0010220 knockdown reduced the abilities of cell migration and invasion in HOS and U2OS cells (Fig. 2F and G). These data indicated that circ_0010220 knockdown repressed osteosarcoma progression *in vitro*.

3.3. Circ_0010220 acts as s sponge for miR-198

As circ_0010220 is mainly located in cytoplasm, we speculated that circ_0010220 may function as a miRNA sponge to mediate the progression of osteosarcoma. To verify this hypothesis, we predicted the targets of circ_0010220 using Circinteractome, and found that miR-198 was a potential target of circ_0010220. The binding site of circ_0010220 and miR-198 was shown in Fig. 3A. To confirm their interaction, we constructed circ_0010220- wt and circ_0010220-mut luciferase reporter vectors. Dual luciferase reporter assay indicated that miR-198 overexpression caused > 70% reduction in luciferase activity of circ_0010220- wt group in contrast with the miR-NC transfection, while it had little effect on circ_0010220-mut group (Fig. 3B). RIP assay uncovered that circ_0010220 and miR-198 were enriched by anti-Ago2, not anti-IgG, which indicating the presence of circ_0010220 and miR-198 in RNA-induced silencing complex (Fig. 3C). Moreover, RNA pull-down assay displayed that circ_0010220 was enriched in bio-miR-198 group compared to miR-NC group (Fig. 3D). Additionally, the effect of circ_0010220 on miR-198 level was analyzed in HOS and U2OS cells. Circ_0010220 overexpression led to > 4.5-fold increase in circ_0010220 expression in the two cells (Fig. 3E). Besides, miR-198 level was negatively regulated by circ_0010220 (Fig. 3F). Furthermore, miR-198 level was markedly decreased in osteosarcoma tissues in comparison to normal samples (n = 51) (Fig. 3G). And miR-198 expression in osteosarcoma tissues (n = 51) was negatively correlated to circ_0010220 level ($P < 0.0001$, $r = -0.8491$) (Fig. 3H). In addition, miR-198 level was significantly declined in HOS and U2OS cells in comparison to hFOB 1.19 cells (Fig. 3I). These results uncovered that miR-198 was lowly expressed in osteosarcoma tissue and cells, and was negatively regulated by circ_0010220.

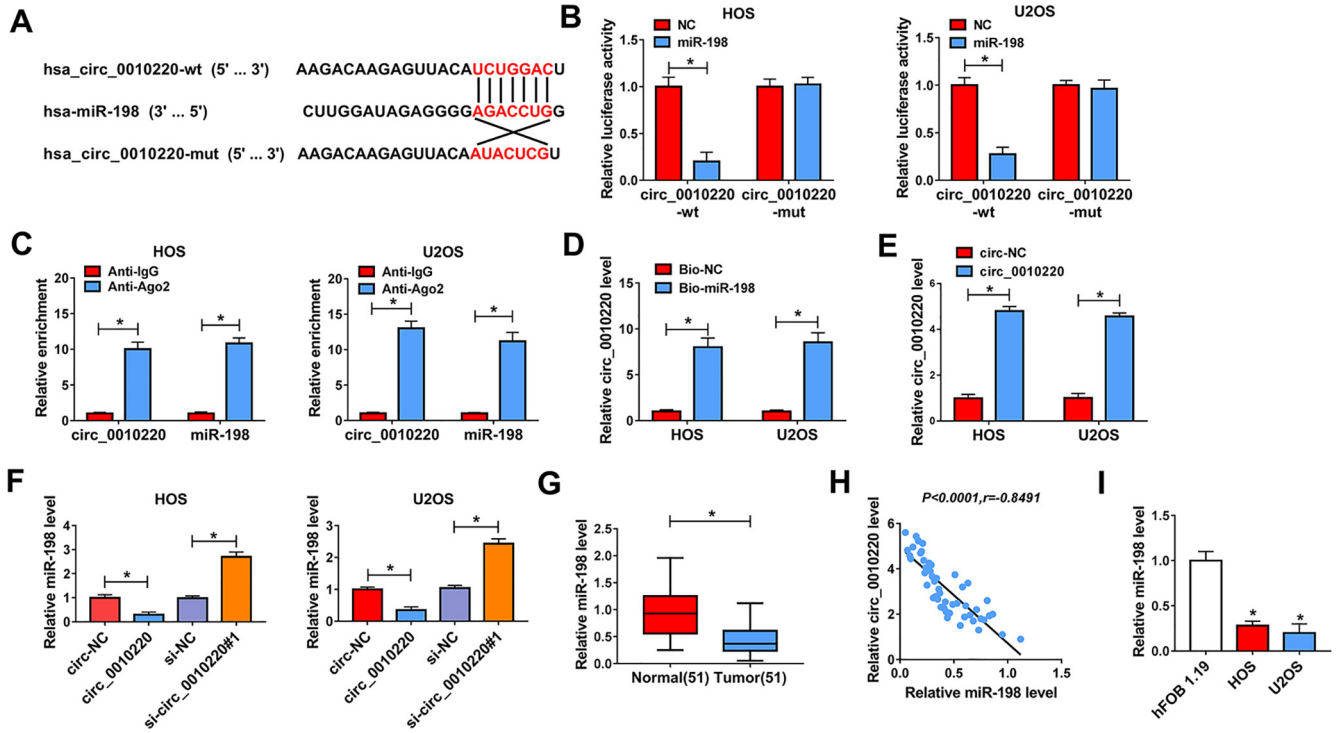

Fig. 3. Circ_0010220 acted as a sponge for miR-198 in osteosarcoma cells. (A) Schematic illustration demonstrated the complementary bind sites of miR-198 in circ_0010220 sequence. (B) Luciferase activity in HOS and U2OS cells co-transfected with circ_0010220- wt or circ_0010220-mut and miR-198 mimic or miR-NC. (C) Ago2 RIP assay for the enrichment of circ_0010220 and miR-198 in cells incubated with anti-IgG or anti-Ago2. (D) RNA pull-down assay were used to measure relative level of circ_0010220 in HOS and U2OS cells incubated with biotinylated miR-198 probe or bio-NC probe. (E) Circ_0010220 expression was examined in cells transfected with circ_0010220 overexpression vector or circ-NC. (F) miR-198 level was detected in cells with transfection of circ-NC, circ_0010220 overexpression vector, si-NC or si-circ_0010220#1. (G) miR-198 level was examined in 51 paired osteosarcoma tissues and adjacent normal tissues (n = 51). (H) Correlation between circ_0010220 and miR-198 expression in 51 cases of osteosarcoma tissues was analyzed by Pearson's correlation analysis. (I) miR-198 level was examined in osteosarcoma cells (HOS, U2OS) and hFOB 1.19 cells. $^{*}P < 0.05$.

3.4. Knockdown of miR-198 partly mitigates the effect of circ_0010220 knockdown on cell proliferation, cell cycle, apoptosis, migration and invasion

To explore whether miR-198 mediated the function of circ_0010220 on osteosarcoma progression, HOS and U2OS cells were transfected with si-NC, si-circ_0010220#1, si-circ_0010220 #1 + anti-NC or si-circ_0010220#1 + anti-miR-198, respectively. The knockdown efficacy of anti-miR-198 on miR-198 level was validated in Fig. 4A. Besides, miR-198 level was elevated by circ_0010220 knockdown, but was weakened by transfection of anti-miR-198 in HOS and U2OS cells (Fig. 4B). Furthermore, miR-198 downregulation attenuated circ_0010220 knockdown-mediated the inhibition effects on cell proliferation (Fig. 4C and D). In addition, miR-198 knockdown partly overturned the effects of circ_0010220 knockdown on cell cycle and apoptosis (Fig. 4E-G). Moreover, miR-198 knockdown rescued circ_0010220 knockdown-mediated suppression on cell migration and invasion (Fig. 4H and I). These results disclosed that circ_0010220 suppressed osteosarcoma progression via regulating miR-198.

3.5. Circ_0010220 upregulated STX6 expression by sponging miR-198 in osteosarcoma cells

To verify the function of circ_0010220/miR-198 axis in osteosarcoma cells, we further predicted the targets of miR-198 via bioinformatics software TargetScan. Eight genes (IGF1R, TRIM44, SOX5, WNT7B, TGM2, XIAP, STX6 and IKBKB) were predicted that might be the targets of miR-198. Next, HOS cells were transfected with miR-NC or miR-198 mimic, and the levels of target genes were evaluated. As shown in Supplementary Fig. 1, elevated expression of miR-198 suppressed the levels of target genes, especially the levels of STX6. Thus, STX6 was chosen for subsequent research. To further investigate if miR-198 binds to the 3′UTR of STX6, the sequences of STX6 3′UTR contained wild type or mutant type miR-198 binding sites were inserted into the luciferase reporter plasmids (STX6-wt and STX6-mut) (Fig. 5A). Dual luciferase reporter assay indicated that miR-198 addition led to > 70% reduction of luciferase activity in STX6-wt group, while this influence was abrogated in STX6-mut group (Fig. 5B). Moreover, RIP analysis displayed that miR-198 and STX6 were enriched by Ago2 RIP (Fig. 5C). Additionally, STX6 protein level was significantly decreased by circ_0010220 knockdown, while this effect was restored by miR-198 knockdown (Fig. 5D). Furthermore, STX6 expression was obviously enhanced in osteosarcoma tissues (n = 51) in comparison to normal samples (n = 51) (Fig. 5E and F). And STX6 level in 51 cases of osteosarcoma tissues was positively associated with circ_0010220 expression ($P < 0.0001$, $r = 0.8068$) (Fig. 5G), and negatively correlated to miR-198 level ($P < 0.0001$, $r = -0.836$) (Fig. 5H). In addition, STX6 protein level was significantly enhanced in HOS and U2OS cells in comparison to hFOB 1.19 cells (Fig. 5I). These data showed that circ_0010220 upregulated STX6 expression via sponging miR-198 in osteosarcoma.

3.6. Overexpression of STX6 partly reversed the effects of miR-198 on cell proliferation, migration, invasion, cell cycle and apoptosis

To investigate the function of miR-198/STX6 axis on osteosarcoma progression *in vitro*, HOS and U2OS cells were transfected

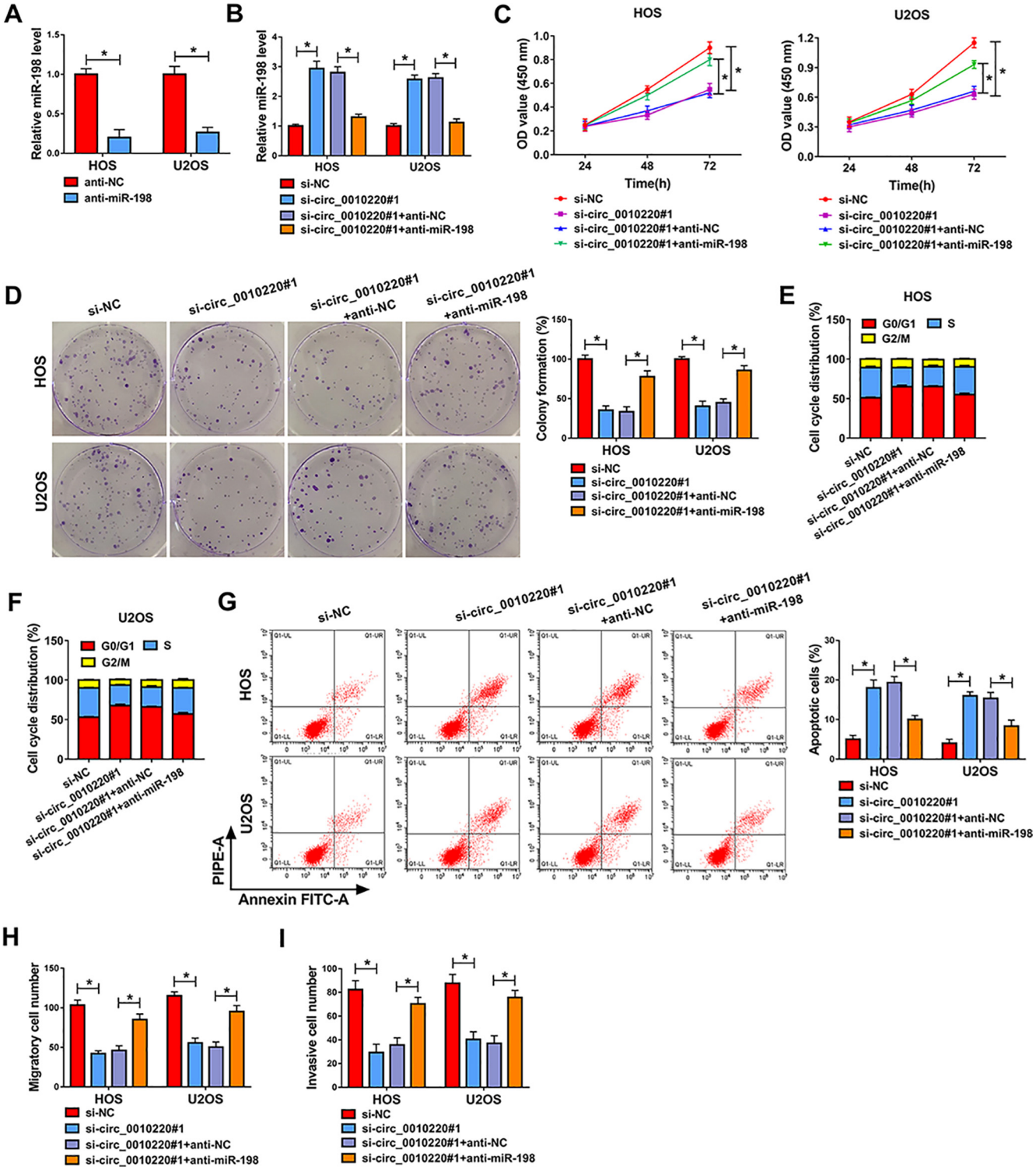

Fig. 4. Knockdown of miR-198 reversed the effect of circ_0010220 knockdown on cell proliferation, cell cycle, apoptosis, migration and invasion in osteosarcoma cells. (A) miR-198 level was examined in HOS and U2OS cells transfected with anti-miR-198 or anti-NC. (B-I) HOS and U2OS cells transfected with si-NC, si-circ_0010220#1, si-circ_0010220#1 + anti-NC, or si-circ_0010220#1 + anti-miR-198, respectively. (B) miR-198 level, (C) cell proliferation, (D) colony formation, (E and F) cycle distribution, (G) apoptosis, (H) migration and (I) invasion were examined in cells upon transfection. $^{*}P < 0.05$.

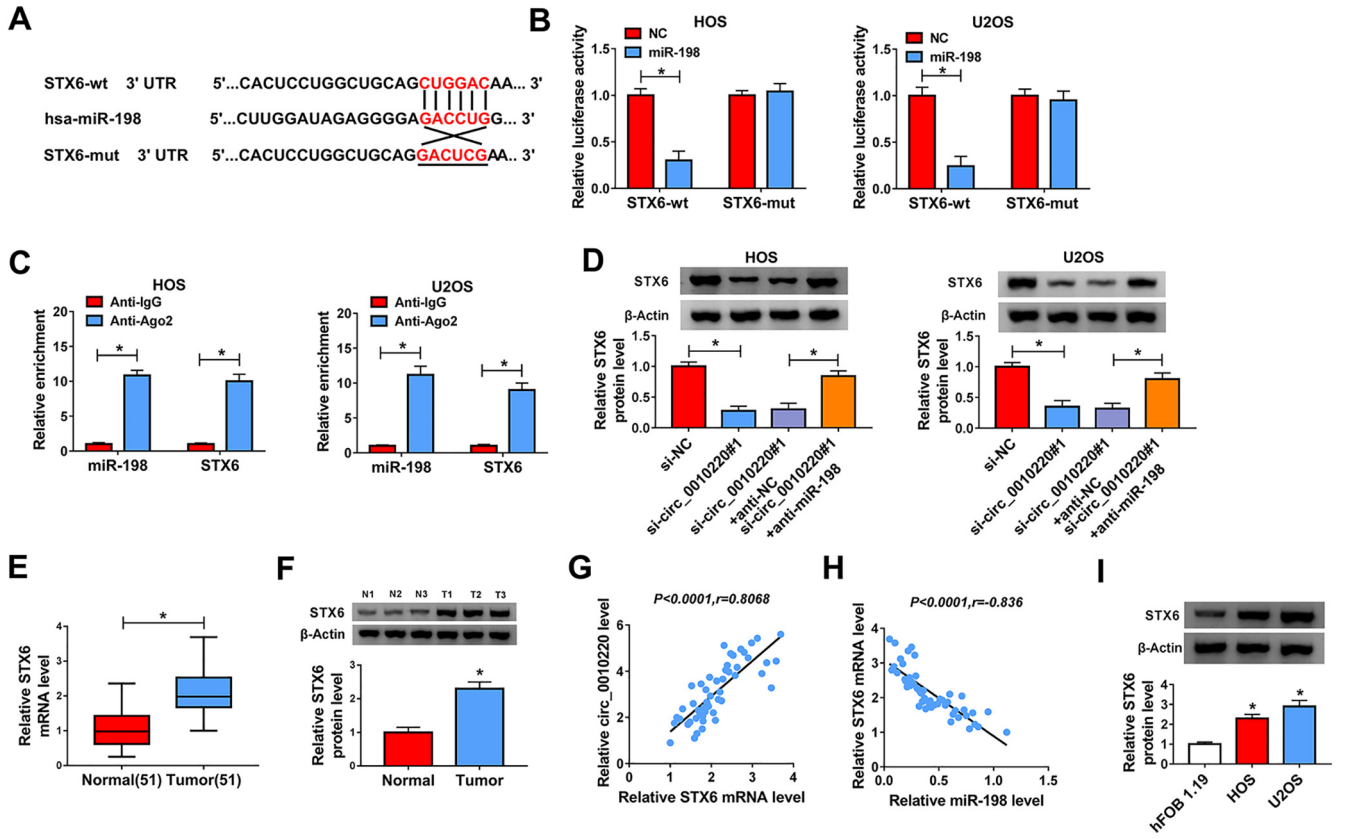

Fig. 5. Circ_0010220 upregulated STX6 expression by sponging miR-198 in osteosarcoma cells. (A) The binding sites between miR-198 and STX6 was predicted by bioinformatics software Targetscan. (B) HOS and U2OS cells were co-transfected with STX6-wt or STX6-mut and miR-198 mimic or miR-NC, luciferase activity was measured using dual-luciferase reporter system. (C) The enrichment of miR-198 and STX6 in cells incubated with anti-IgG or anti-Ago2 were measured. (D) STX6 protein level was examined in cells transfected with si-NC, si-circ_0010220#1, si-circ_0010220#1 + anti-NC, or circ_0010220#1 + anti-miR-198. (E and F) STX6 mRNA and protein levels were examined in 51 paired of osteosarcoma tumor tissues and adjacent normal tissues. (G and H) The correlation between STX6 expression and circ_0010220 or miR-198 levels in 51 cases of osteosarcoma tissues was analyzed by Pearson's correlation analysis. (I) STX6 protein level was detected in osteosarcoma cells (HOS, U2OS) and hFOB 1.19 cells. $^{*}P < 0.05$.

with NC, miR-198 mimic, miR-198 mimic + pcDNA, or miR-198 mimic + STX6 overexpression vector. As shown in Fig. 6A, miR-198 level was elevated more than five times by miR-198 mimic transfection. STX6 protein level was significantly reduced by miR-198 overexpression, while it was restored by introduction of STX6 overexpression vector (Fig. 6B). Moreover, miR-198 overexpression repressed cell proliferation, and this effect was abolished by STX6 overexpression (Fig. 6C and D). Additionally, miR-198 overexpression obviously induced cycle arrest at G0/G1 phase and apoptosis promotion, which was weakened by STX6 up-regulation (Fig. 6E–G). Furthermore, miR-198 markedly restrained cell migration and invasion, while it was relieved by addition of STX6 (Fig. 6H and I). These data suggested that miR-198 repressed osteosarcoma progression via targeting STX6.

3.7. Circ_0010220 knockdown suppressed the growth of osteosarcoma cells in vivo

To explore the functions of circ_0010220 *in vivo*, a xenograft tumor model was established. Stable U2OS cells transfected with Lenti-sh-circ_0010220 or Lenti-sh-NC were subcutaneous injected into the right armpit of nude mice (n = 5 per group). As shown in Fig. 7A and B, xenograft tumors derived from circ_0010220-depletion cells were notably reduced in tumor volume and weight in comparison with Lenti-sh-NC group. Furthermore, circ_0010220, miR-198, STX6 and PCNA (a proliferation-related biomarker) levels were measured in xenograft tumor tissues, and results indicated that circ_0010220, STX6 and PCNA levels were significantly reduced, while miR-198 expression was enhanced in Lenti-sh-circ_0010220 group (Fig. 7C and D). Furthermore, IHC staining assay for ki-67 indicated that the percentage of ki-67 positive cells was decreased in circ_0010220-depletion group in contrast with the lenti-sh-NC group (Fig. 7E), which indicated that circ_0010220 knockdown suppressed the proliferation of osteosarcoma cells *in vivo*.

4. Discussion

Osteosarcoma is a common bone tumor in children and young adults [24]. The prognosis of osteosarcoma patients remains poor despite the 5-year survival rate of osteosarcoma patients having increased in the past 30 years [25]. It is urgently needed to search novel diagnostic and therapeutic targets for osteosarcoma therapy.

In recent years, circRNAs cached the attention of researchers owing to its stable structure, and cell and tissue specificity, as well as its stable expression in saliva, blood and exosomes [26], which might be a potential target for the diagnosis and treatment of multiple diseases, including cancer [27,28]. Increasing evidence has uncovered that the dysregulation of circRNAs in multiple cancers is closely related to the development and metastasis of tumors, which could be used as the therapeutic target for osteosarcoma [29]. Previous evidence reported that multiple circRNAs could play oncogenic roles in osteosarcoma progression by promoting cell proliferation, migration and invasion, including hsa_circ_0003732,

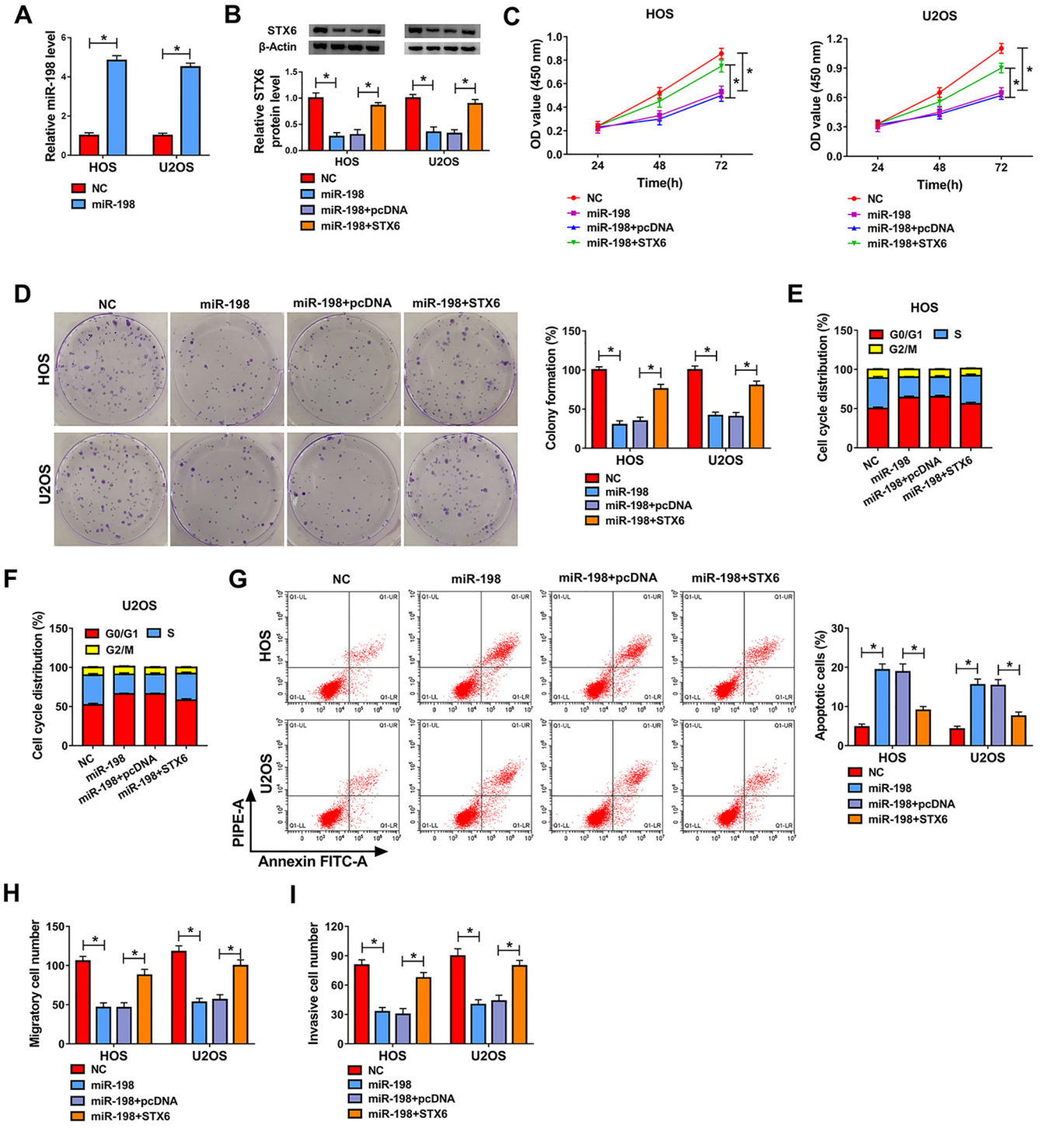

Fig. 6. STX6 mediated the tumor-suppressive role of miR-198 in osteosarcoma cells. (A) miR-198 expression was detected in HOS and U2OS cells with transfection of miR-198 mimic or miR-NC. STX6 protein level (B), cell proliferation (C), colony formation (D), cycle distribution (E and F), apoptosis (G), migration (H) and invasion (I) were measured in cells with transfection of NC, miR-198 mimic, miR-198 mimic + pcDNA or miR-198 mimic + STX6 overexpression vector. *$P < 0.05$.

hsa_circ_0005909, hsa_circ_0000073, hsa_circ_0136666, hsa_circ_001621 and hsa_circ_0008792 [14–16,30–32]. We selected a novel circRNA circ_0010220 based on GSE140256 dataset, a microarray profiling analysis of circRNAs expression in osteosarcoma. Our study confirmed that circ_0010220 was upregulated in osteosarcoma tumor and cells, and it was associated with the poor survival of osteosarcoma patients. Moreover, loss-of-function experiments indicated that circ_0010220 knockdown suppressed cell proliferation, migration and invasion but induced cell cycle arrest and apoptosis in osteosarcoma cells. Besides, the xenograft model is commonly used for the pre-clinical study on osteosarcoma [33]. Here we established a xenograft tumor model of human osteosarcoma in nude mice, and further identified that circ_0010220 knockdown curbed the growth of xenograft tumor *in vivo*.

These research indicated that circ_0010220 functions as a tumor promoter in osteosarcoma, which might be a potential target for the treatment of osteosarcoma.

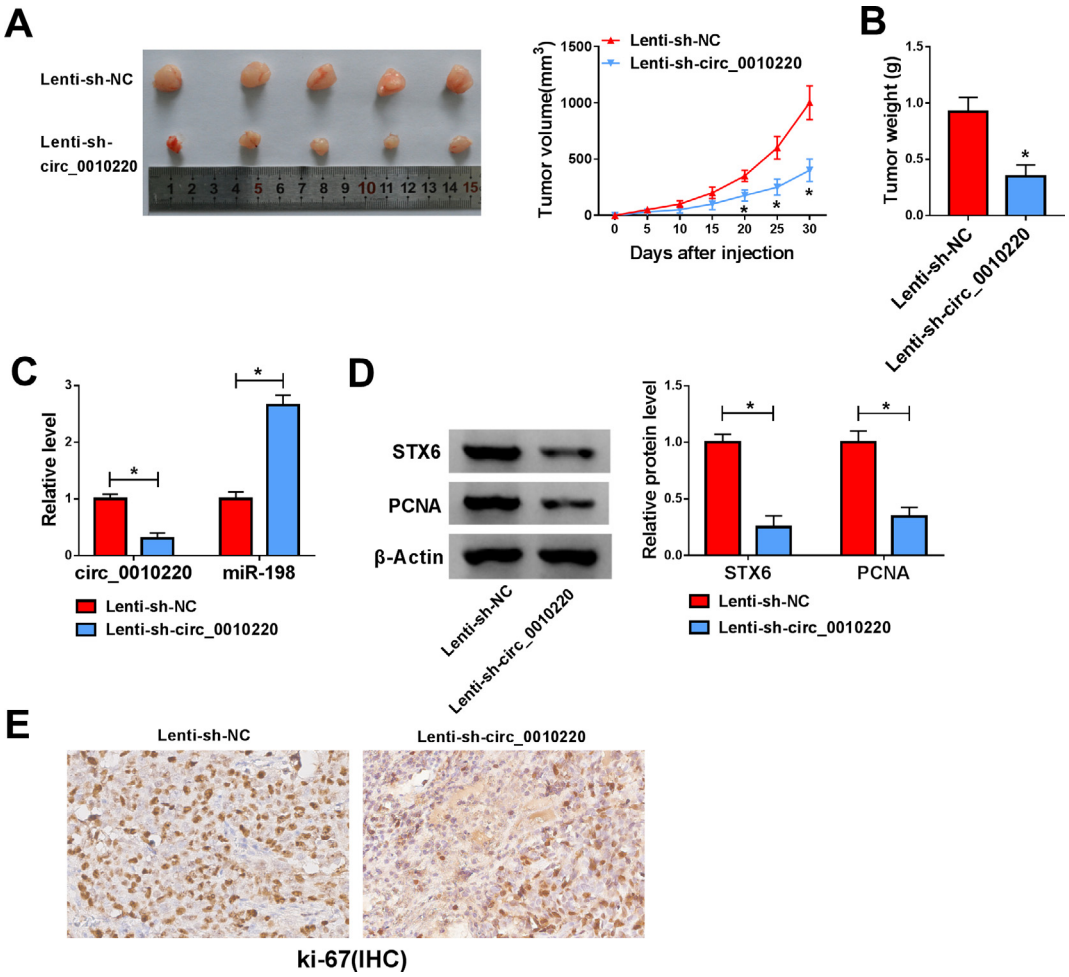

Fig. 7. Circ_0010220 knockdown suppressed the growth of osteosarcoma cells *in vivo*. (A) Nude mice were injected 3 × 10^6 stable U2OS cells transfected with Lenti-sh-circ_0010220 or Lenti-sh-NC (five mice for each group). Tumor volume was measured every 5 days. 30 days upon injection, tumors were dissected and photographed. (B) Tumor weight at the end of the experiment (day 35). (C and D) Circ_0010220, miR-198, STX6 and PCNA levels were measured in xenograft tumor tissues (n = 5 per group). (E) IHC staining for ki-67 in xenograft tumor tissues (five mice for each group). *$P < 0.05$.

The circRNA/miRNA/mRNA network is a popular mechanism underlying the function of circRNA in osteosarcoma [34]. Our study revealed that miR-198 was a target of circ_0010220 and was negatively regulated by circ_0010220. A lot of research has displayed that miR-198 could serve as a suppressor in various tumors, including papillary thyroid cancer, gastric cancer and esophageal cancer [35–37]. More importantly, Zhang *et al.* reported miR-198 constrained osteosarcoma cell proliferation, migration and invasion via reducing ROCK1, and low expression of miR-198 indicated the poor outcomes of patients [38]. Furthermore, Georges et al. suggested miR-198 level was reduced in osteosarcoma, and associated with tumor metastasis [39]. These reports suggested that miR-198 played a tumor-suppressive role in osteosarcoma. Similarly, we also validated that miR-198 functions as a tumor suppressor in osteosarcoma. Overexpression of miR-198 obviously reversed the malignant phenotype of osteosarcoma cells, suppressed the proliferation, migration and invasion, but induced cell cycle arrest and apoptosis in osteosarcoma cells. Furthermore, our research disclosed that circ_0010220 exerted its regulatory functions in osteosarcoma progression through harboring miR-198.

Further investigation validated that STX6 was a target of miR-198 in osteosarcoma. Riggs *et al.* showed that STX6 could promote chemotactic cell migration [40]. Moreover, STX6 contributed to cell proliferation and migration in esophageal squamous cell carcinoma [41]. More importantly, STX6 facilitated osteosarcoma cell proliferation, migration and invasion via activating the Wnt/β-catenin pathway [42]. Consistent with previous research, we also identified the carcinogenic function of STX6 in osteosarcoma, and found that miR-198 exerted the inhibitive role via decreasing STX6. In addition, we confirmed that circ_0010220 upregulated STX6 expression by sponging miR-198, thereby mediating cell proliferation, migration, invasion, cell cycle progression and apoptosis in osteosarcoma.

In conclusion, circ_0010220 was upregulated in osteosarcoma and modulated miR-198/STX6 axis to regulate the progression of osteosarcoma *in vitro* and *in vivo*. Our research proposes a novel insight into the pathology of osteosarcoma, and provides a novel target for osteosarcoma treatment.

Declaration of Competing Interest

The authors declare that they have no known competing financial interests or personal relationships that could have appeared to influence the work reported in this paper.

Acknowledgement

None.

Funding

This research was supported by Henan Province Science and Technology Research Project (202102310458).

Appendix A. Supplementary data

Supplementary data to this article can be found online at https://doi.org/10.1016/j.jbo.2021.100360.

References

[1] J.L. Ferguson, S.P. Turner, Bone cancer: diagnosis and treatment principles, Am. Fam. Physician 98 (4) (2018) 205–213.
[2] S.C. Kaste, C.B. Pratt, A.M. Cain, D.J. Jones-Wallace, B.N. Rao, Metastases detected at the time of diagnosis of primary pediatric extremity osteosarcoma at diagnosis: imaging features, Cancer 86 (8) (1999) 1602–1608.
[3] G.N. Yan, Y.F. Lv, Q.N. Guo, Advances in osteosarcoma stem cell research and opportunities for novel therapeutic targets, Cancer Lett. 370 (2) (2016) 268–274.
[4] B.A. Lindsey, J.E. Markel, E.S. Kleinerman, Osteosarcoma overview, Rheumatol. Ther. 4 (1) (2017) 25–43.
[5] L.S. Kristensen, M.S. Andersen, L.V.W. Stagsted, K.K. Ebbesen, T.B. Hansen, J. Kjems, The biogenesis, biology and characterization of circular RNAs, Nat. Rev. Genet. 20 (11) (2019) 675–691.
[6] Y. Zhang, W. Xue, X. Li, J. Zhang, S. Chen, J.L. Zhang, L. Yang, L.L. Chen, The biogenesis of nascent circular RNAs, Cell Rep. 15 (3) (2016) 611–624.
[7] S. Qu, X. Yang, X. Li, J. Wang, Y. Gao, R. Shang, W. Sun, K. Dou, H. Li, Circular RNA: a new star of noncoding RNAs, Cancer Lett. 365 (2) (2015) 141–148.
[8] Z.J. Zhao, J. Shen, Circular RNA participates in the carcinogenesis and the malignant behavior of cancer, RNA Biol. 14 (5) (2017) 514–521.
[9] I.L. Patop, S. Kadener, circRNAs in Cancer, Curr. Opin. Genet. Dev. 48 (2018) 121–127.
[10] J. Jin, A. Chen, W. Qiu, Y. Chen, Q. Li, X. Zhou, D. Jin, Dysregulated circRNA_100876 suppresses proliferation of osteosarcoma cancer cells by targeting microRNA-136, J. Cell. Biochem. 120 (9) (2019) 15678–15687.
[11] J. Liu, L. Yang, Q. Fu, S. Liu, Emerging roles and potential biological value of CircRNA in osteosarcoma, Front. Oncol. 10 (2020) 552236.
[12] B. Wan, H. Hu, R. Wang, W. Liu, D. Chen, Therapeutic potential of circular RNAs in osteosarcoma, Front. Oncol. 10 (2020) 370.
[13] X. Huang, W. Yang, Z. Zhang, Z. Shao, Dysregulated circRNAs serve as prognostic and diagnostic markers in osteosarcoma by sponging microRNA to regulate the downstream signaling pathway, J. Cell. Biochem. 121 (2) (2020) 1834–1841.
[14] L. Li, X.A. Kong, M. Zang, J. Dong, Y. Feng, B. Gui, Y. Hu, Hsa_circ_0003732 promotes osteosarcoma cells proliferation via miR-545/CCNA2 axis, Biosci. Rep. 40 (6) (2020).
[15] S. Ding, G. Zhang, Y. Gao, S. Chen, C. Cao, Circular RNA hsa_circ_0005909 modulates osteosarcoma progression via the miR-936/HMGB1 axis, Cancer Cell Int. 20 (2020) 305.
[16] X. Li, Y. Liu, X. Zhang, J. Shen, R. Xu, Y. Liu, X. Yu, Circular RNA hsa_circ_0000073 contributes to osteosarcoma cell proliferation, migration, invasion and methotrexate resistance by sponging miR-145-5p and miR-151-3p and upregulating NRAS, Aging (Albany NY) 12 (14) (2020) 14157–14173.
[17] J. Li, F. Zhang, H. Li, F. Peng, Z. Wang, H. Peng, J. He, Y. Li, L. He, L. Wei, Circ_0010220-mediated miR-503-5p/CDCA4 axis contributes to osteosarcoma progression tumorigenesis, Gene 763 (2020) 145068.
[18] M. Qiu, W. Xia, R. Chen, S. Wang, Y. Xu, Z. Ma, W. Xu, E. Zhang, J. Wang, T. Fang, J. Hu, G. Dong, R. Yin, J. Wang, L. Xu, The circular RNA circPRKCI promotes tumor growth in lung adenocarcinoma, Cancer Res. 78 (11) (2018) 2839–2851.
[19] M. Zhang, N. Huang, X. Yang, J. Luo, S. Yan, F. Xiao, W. Chen, X. Gao, K. Zhao, H. Zhou, Z. Li, L. Ming, B. Xie, N. Zhang, A novel protein encoded by the circular form of the SHPRH gene suppresses glioma tumorigenesis, Oncogene 37 (13) (2018) 1805–1814.
[20] R. Sen, S. Ghosal, S. Das, S. Balti, J. Chakrabarti, Competing endogenous RNA: the key to posttranscriptional regulation, Scientific World J. 2014 (2014) 896206.
[21] K.P. Zhu, C.L. Zhang, X.L. Ma, J.P. Hu, T. Cai, L. Zhang, Analyzing the interactions of mRNAs and ncRNAs to predict competing endogenous RNA networks in osteosarcoma chemo-resistance, Mol. Ther. 27 (3) (2019) 518–530.
[22] Z. Wang, M. Deng, L. Chen, W. Wang, G. Liu, D. Liu, Z. Han, Y. Zhou, Circular RNA Circ-03955 promotes epithelial-mesenchymal transition in osteosarcoma by regulating miR-3662/metadherin pathway, Front. Oncol. 10 (2020) 545460.
[23] S. Li, Y. Pei, W. Wang, F. Liu, K. Zheng, X. Zhang, Circular RNA 0001785 regulates the pathogenesis of osteosarcoma as a ceRNA by sponging miR-1200 to upregulate HOXB2, Cell Cycle 18 (11) (2019) 1281–1291.
[24] R.A. Durfee, M. Mohammed, H.H. Luu, Review of osteosarcoma and current management, Rheumatol. Ther. 3 (2) (2016) 221–243.
[25] S.S. Bielack, B. Kempf-Bielack, G. Delling, G.U. Exner, S. Flege, K. Helmke, R. Kotz, M. Salzer-Kuntschik, M. Werner, W. Winkelmann, A. Zoubek, H. Jürgens, K. Winkler, Prognostic factors in high-grade osteosarcoma of the extremities or trunk: an analysis of 1,702 patients treated on neoadjuvant cooperative osteosarcoma study group protocols, J. Clin. Oncol. 20 (3) (2002) 776–790.
[26] D. Liang, D.C. Tatomer, Z. Luo, H. Wu, L. Yang, L.L. Chen, S. Cherry, J.E. Wilusz, The output of protein-coding genes shifts to circular RNAs when the pre-mRNA processing machinery is limiting, Mol. Cell 68 (5) (2017) 940–954.e943.
[27] I. Legnini, G. Di Timoteo, F. Rossi, M. Morlando, F. Briganti, O. Sthandier, A. Fatica, T. Santini, A. Andronache, M. Wade, P. Laneve, N. Rajewsky, I. Bozzoni, Circ-ZNF609 is a circular RNA that can be translated and functions in myogenesis, Mol. Cell 66 (1) (2017) 22–37.e29.
[28] L.S. Kristensen, T.B. Hansen, M.T. Venø, J. Kjems, Circular RNAs in cancer: opportunities and challenges in the field, Oncogene 37 (5) (2018) 555–565.
[29] C. Tu, J. He, L. Qi, X. Ren, C. Zhang, Z. Duan, K. Yang, W. Wang, Q. Lu, Z. Li, Emerging landscape of circular RNAs as biomarkers and pivotal regulators in osteosarcoma, J. Cell. Physiol. (2020).
[30] C. Zhang, H. Zhou, K. Yuan, R. Xie, C. Chen, Overexpression of hsa_circ_0136666 predicts poor prognosis and initiates osteosarcoma tumorigenesis through miR-593-3p/ZEB2 pathway, Aging (Albany NY) 12 (11) (2020) 10488–10496.
[31] X. Ji, L. Shan, P. Shen, M. He, Circular RNA circ_001621 promotes osteosarcoma cells proliferation and migration by sponging miR-578 and regulating VEGF expression, Cell Death Dis. 11 (1) (2020) 18.
[32] L. Chen, Y. Shan, H. Zhang, H. Wang, Y. Chen, Up-regulation of Hsa_circ_0008792 inhibits osteosarcoma cell invasion and migration and promotes apoptosis by regulating Hsa-miR-711/ZFP1, Onco Targets Ther. 13 (2020) 2173–2181.
[33] V.B. Sampson, D.F. Kamara, E.A. Kolb, Xenograft and genetically engineered mouse model systems of osteosarcoma and Ewing's sarcoma: tumor models for cancer drug discovery, Expert Opin. Drug Discov. 8 (10) (2013) 1181–1189.
[34] Y. Qiu, C. Pu, Y. Li, B. Qi, Construction of a circRNA-miRNA-mRNA network based on competitive endogenous RNA reveals the function of circRNAs in osteosarcoma, Cancer Cell Int. 20 (2020) 48.
[35] W. Liu, J. Zhao, M. Jin, M. Zhou, circRAPGEF5 contributes to papillary thyroid proliferation and metastatis by regulation miR-198/FGFR1, Mol. Ther. Nucl. Acids 14 (2019) 609–616.
[36] J. Gu, X. Li, H. Li, Z. Jin, J. Jin, MicroRNA-198 inhibits proliferation and induces apoptosis by directly suppressing FGFR1 in gastric cancer, Biosci. Rep. 39 (6) (2019).
[37] Y. Shi, N. Fang, Y. Li, Z. Guo, W. Jiang, Y. He, Z. Ma, Y. Chen, Circular RNA LPAR3 sponges microRNA-198 to facilitate esophageal cancer migration, invasion, and metastasis, Cancer Sci. (2020).
[38] S. Zhang, Y. Zhao, L. Wang, MicroRNA-198 inhibited tumorous behaviors of human osteosarcoma through directly targeting ROCK1, Biochem. Biophys. Res. Commun. 472 (3) (2016) 557–565.
[39] S. Georges, L.R. Calleja, C. Jacques, M. Lavaud, B. Moukengue, F. Lecanda, T. Quillard, M.T. Gabriel, P.F. Cartron, M. Baud'huin, F. Lamoureux, D. Heymann, B. Ory, Loss of miR-198 and -206 during primary tumor progression enables metastatic dissemination in human osteosarcoma, Oncotarget 9 (87) (2018) 35726–35741.
[40] K.A. Riggs, N. Hasan, D. Humphrey, C. Raleigh, C. Nevitt, D. Corbin, C. Hu, Regulation of integrin endocytic recycling and chemotactic cell migration by syntaxin 6 and VAMP3 interaction, J. Cell Sci. 125 (Pt 16) (2012) 3827–3839.
[41] J. Du, X. Liu, Y. Wu, J. Zhu, Y. Tang, Essential role of STX6 in esophageal squamous cell carcinoma growth and migration, Biochem. Biophys. Res. Commun. 472 (1) (2016) 60–67.
[42] P.R. Zhang, J. Ren, J.S. Wan, R. Sun, Y. Li, Circular RNA hsa_circ_0002052 promotes osteosarcoma via modulating miR-382/STX6 axis, Hum. Cell 33 (3) (2020) 810–818.